

Microwave Assisted Sintering of Sr-doped Zinc Titanate ($\text{Sr}_{0.2}\text{Zn}_{0.8}\text{TiO}_3$) Nano-ceramics

Guru Sampath Kumar ANKISETTY^{1*}, Vijay Kumar JINDE², Mahesh Kumar UNGARALA³, Siva Kumar PENDYALA⁴, Obulapathi LAVULURI⁵, Sharon Samyuktha VADDE⁶

¹ Department of H & S (Physics), Malla Reddy Engineering College (A), Secunderabad, T.S.-500100, India

² Department of H&S (Physics), SKU College of Engg.&Tech., Sri Krishnadevaraya University, Anantapur, A.P.-515003, India

³ Department of H&S (Physics), Srinivasa Ramanujan Institute of Technology (A), Anantapur, A.P.-515701, India

⁴ Department of H & S (Physics), St. Peter's Engineering College (A), Secunderabad, T.S.-500100, India

⁵ Department of H & S (Physics), Annamacharya Institute of Tech. & Sci's (A), Rajampet, A.P.-516126, India

⁶ Department of Physics, Maris Stella College (Autonomous), Vijayawada, A.P.-520008, India

<http://doi.org/10.5755/j02.ms.33625>

Received 13 March 2023; accepted 6 June 2023

$\text{Sr}_{0.2}\text{Zn}_{0.8}\text{TiO}_3$ (SZT) ternary nanopowders of perovskite structure samples were prepared by conventional solid state reaction technique using ultra-pure metal oxide powders. SrCO_3 , ZnO and TiO_2 powders were used as a source of Strontium, Zinc, and Titanium. The calcination temperature of the samples is 820 °C and sintered at different temperatures ranging from 850 °C to 1000 °C in conventional and microwave furnaces for 2 hours and 30 min., respectively. The synthesized nano-powders were characterized using XRD, SEM, XPS and their dielectric properties were studied by temperature dependent LCR meter. The dielectric constant increases with an increase in sintering temperature until 950 °C and it decreases with a further increase of frequency.

Keywords: SZT ceramics, ilmenite hexagonal structure, sintering temperature, XPS, dielectric constant.

1. INTRODUCTION

Microwave dielectric ceramics improve device efficiency and the packaging density of microwave integrated circuits and are widely used in microwave filters, oscillators and phase shifters. With the rapid development of the fifth-generation (5G) mobile network and the need for new microwave (MW) devices, it is necessary to explore novel materials for rapid signals [1]. Dielectric constant (k) and loss tangent (δ) values play a vital role in microwave and millimeter-wave (30–300 GHz) radio frequencies as circuit substrates and other device applications, due to their less time delay in signal transmission [2]. In general, MW ceramics are synthesized by using conventional sintering at temperatures greater than 1,200 K [3, 4].

The high- k dielectric materials are important components in microelectronic devices such as flash memory, dynamic random-access memory (DRAM) and central processing unit (CPU) due to their good capacitive coupling, reduction in leakage current between electrodes and less energy consumption for long-term reliability (flash memory) [5]. Wide band gap (E_g) is also an important parameter in addition to the dielectric constant to reduce the charge carrier injection from electrodes into dielectrics that causes the leakage current. Therefore, the ideal dielectric with high- k should possess both large k and E_g [6]. The k was dependent on the ionic polarizabilities of any doped ATiO_3 structured ceramics (Sr, Mn, Zn, Mg) [7]. K. Yim. et al. [8] reported that the doped ZnTiO_3 is an attractive dielectric material having good physical

(dielectric) properties at a high frequency range ($\epsilon_r = 25$, $\tan(\delta) < 10^{-3}$, $\tau_f = \sim -51$ ppm/°C) and its comparatively low sintering temperature (below 1000 °C), high Q-factor is the result of ordered behavior and in the case of doped ZnTiO_3 and due to compositional ordering as a result of the decrease in the lattice strain [9, 10]. A good dielectric material must have controlled grain size, be less porous, and be highly textured. The dielectric constant increases with doping concentration and sintering environment (microwave) [11]. Therefore, high dielectric constant (k) and low loss $\tan(\delta)$ are key parameters in identifying the suitable dielectric material which is an extremely challenging task. Recently, Maddaiah M. et al. [12] introduced Sr-doped MnTiO_3 rutile ceramics with high k ($> 10^3$) and low $\tan(\delta)$ (< 0.05) over a wide temperature range between 300 ~ 450 K. Lin L., et. al [13] and Pallavi S., et. al [14] reported that dielectric properties of titanate ceramics greatly depended on the Sr doping concentration and sintering temperature. The optimum doping concentration and sintering temperature about 0.2 to 0.3 wt.% and 950 °C. Compared with MnTiO_3 , Sr-doped ZnTiO_3 ceramics have much more stable physical (dielectric) properties [15]. Based on the above discussion, we choose ZnTiO_3 as the base while SrCO_3 substitutes dopant for base materials and the overall charge is balanced with proper stoichiometric ratio.

In the present work, a stoichiometric compound of $\text{Sr}_{0.2}\text{Zn}_{0.8}\text{TiO}_3$ were prepared by conventional solid state reaction, following the estimation of the structure of the compound, lattice parameters, grain size and surface

* Corresponding author. Tel.: +91 9985102547; fax: +91-9390254331.
E-mail: sampathkumar.phy@mrec.ac.in (G.S.K. Ankisetty)

morphology, composition, and dielectric properties were analyzed based on different characterizations.

2. EXPERIMENTAL DETAILS

$\text{Sr}_{0.2}\text{Zn}_{0.8}\text{TiO}_3$ ceramic compound was synthesized by standard solid-state reaction technique using analytical grade powders of ZnO, SrCO_3 , and TiO_2 (purity > 99.99 %). The powders were calcined at 500 °C for Two hours and chilled in dry circumstances to eliminate any remaining moisture. In a panner ball mill, the stoichiometric powders of SrCO_3 , ZnO and TiO_2 were combined and crushed for 5 hours using ethanol as the gaining medium. To form the precursor powder, the mixture was first dried at 100 °C for 5 hours and then calcined at 820 °C for 5 hours. The calcined powder was remilled with zirconia balls for 5 hours in ethanol after being sieved through a 200 μm sieve, and then dried. The resulting composite was then crushed and pressed into disc pellets by a cold isostatic press at a pressure of 200 MPa, with a diameter of 1.2 cm and a thickness of 2 to 6 mm. Finally, the synthesized samples were sintered in a conventional furnace and microwave furnace at 850–1000 °C for 2 hours and 30 minutes, respectively.

The crystalline phase of the ceramic samples was studied at room temperature by an automated X-ray diffractometer (D/Max-3C, Rigaku, Japan) over the 2 θ range of 10–80° with a step of 0.02° and a step time of 10 s. The microstructures and surface morphology of the ceramic were investigated with a scanning electron microscope (SEM, JSM-6500F, JEOL, Japan). The sample composition and spin states were measured by XPS analysis. The dielectric properties (k & $\tan(\delta)$) were measured using the HIOKI 3532-50 LCR HiTester (Japan) at varying temperatures and frequencies (up to 1 MHz).

3. RESULTS AND DISCUSSION

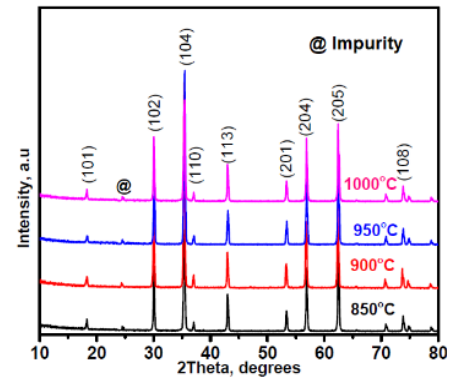
The XRD patterns of conventional and microwave sintered $\text{Sr}_{0.2}\text{Zn}_{0.8}\text{TiO}_3$ ceramic samples are shown in Fig. 1. The patterns predominantly show diffraction peaks associated with the ilmenite hexagonal structure with a space group of $R\bar{3}$ [16]. Furthermore, in conventional sintered samples, there were secondary peaks attributed to ZnTiO_3 (JCPDS file #26-1500) [17] as Zn_2TiO_4 (JCPDS file #86-0158), while in microwave sintering, Zn^{2+} is substituted by Sr^{2+} ions. The incorporation of Sr ions into the ZnTiO_3 lattice is known to be able to suppress the phase transition from anatase to the rutile phase [18]. This phenomenon results from the formation of the Ti-O- Sr^{2+} bonds, leading to the stabilization of the hexagonal phase in ZnTiO_3 [19].

It can also be due to this low sintering temperature and short soaking time during microwave sintering, which can effectively avoid liquid segregation at grain boundaries of the SZT ceramics that occurs with other sintering methods [20]. The average crystallite size is estimated by using Debye-Scherrer's method [21]:

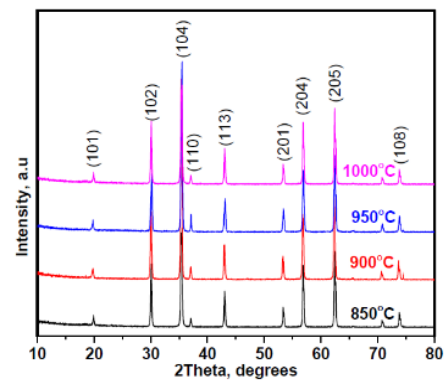
$$D = \frac{0.9 \cdot \lambda}{\beta \cos \theta}, \quad (1)$$

where D is the average crystallite size; λ is the wavelength (1.5404 Å [22]) of X-rays used; β is the full width at half

maxima (FWHM) in radians. The calculated average crystallite size of Sr-doped ZnTiO_3 is increased with sintering temperature till 950 °C (31.5–46.8 nm) later it slightly decreases (38.3 nm).



a



b

Fig. 1. X-ray diffraction patterns of SZT ceramics at various sintering temperatures (850–1000 °C): a–conventional sintering; b–microwave sintering

It is noticed that the normal crystallite size reduction happens at high temperatures. This is because of the difference in the development rate between various crystallographic planes [23].

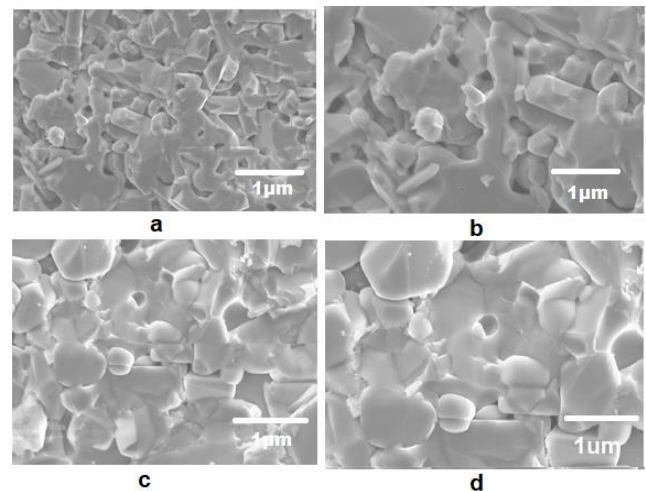


Fig. 2. Surface morphology of SZT ceramics microwave sintered at: a–850 °C; b–900 °C; c–950 °C; d–1000 °C

Fig. 2 depicts the SEM images of microwave-assisted SZT ceramic samples sintered at 850–1000 °C, respectively. All the SZT samples' grains are crystalline, and neither a clear secondary phase nor any segregation phenomena are discernible [24]. For the samples presented in Fig. 2, the average grain sizes were determined to be 1.28, 1.48, 1.67, and 1.42 μm , respectively. We think that microwave sintering may modify the microstructure and dielectric characteristics of the SZT ceramics by the contact between the particles and grain development during the sintering process [25]. XPS was used to examine the chemical composition of the SZT ceramic samples. The SZT@950°C ceramic sample's global survey scan is displayed in Fig. 3. As a result, XPS data support the incorporation of Sr elements into the ZnTO_3 lattice (SZT).

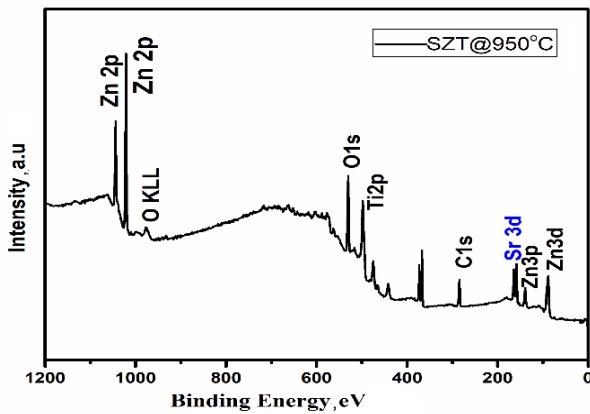


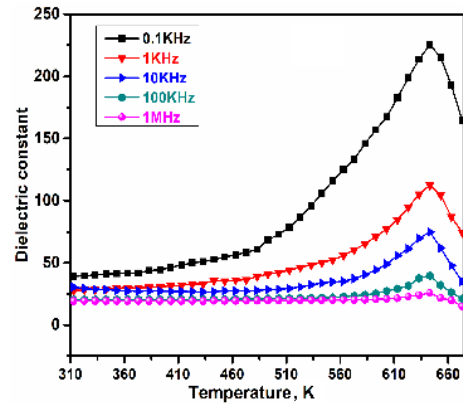
Fig. 3. XPS global survey scan of microwave-sintered SZT ceramics at 950 °C

The variation of dielectric constant (k) and dielectric loss tangent ($\tan(\delta)$) with temperature (300–700K) at different frequencies (1 kHz to 1 MHz) of the SZT@950 °C ceramic sample is shown in Fig. 4. It can be observed from Fig. 4, that the k (Fig. 4 a) and $\tan(\delta)$ (Fig. 4 b) is found to increase slowly with the increase of temperature up to 500 K and above 500 K, a sharp increasing trend in both cases is observed for all the samples. The sharp increase can be attributed to the interfacial or space-charge polarization effect [26]. In addition, k and $\tan(\delta)$ were found to decrease with an increase in frequency. This happens due to ineffective space charges at the grain boundary interface [27, 28].

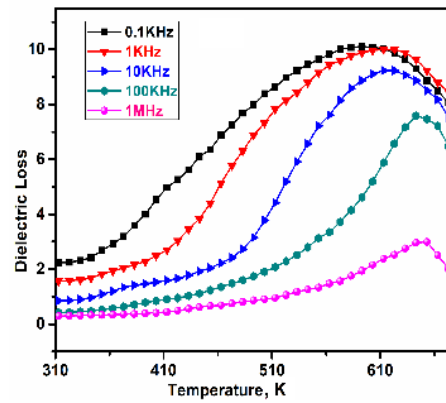
At room temperature ($f = 1$ MHz), the SZT ceramic sintered at 950 °C showed a dielectric constant of ~ 25 . In general, the polarization due to grain boundaries is more active at the lower frequencies, and as the frequency increase, the polarization due to grains will be more. Up to 100 Hz, the Maxwell-Wagner interfacial polarization [29] becomes predominant and for further increase of frequency, the effectiveness of space charges will be diminished. Thus, the k , as well as $\tan(\delta)$, will be decreased. The transition temperature of the SZT@950 °C is noticed at ~ 655 K at which the structural transformation usually occurs. Normally, at the transition temperature, all the charge carriers will be accumulated at the grain boundary interface and therefore the resistivity of the grain boundary decreases. Hence, the breakage of the grain boundary takes place which can again be responsible for the peak value of the

dielectric constant or loss [12, 30].

Fig. 5 shows the dielectric constant and loss of SZT specimens with respect to microwave sintering temperature at RT and $f = 1$ MHz. With the increase in the sintering temperature, the K of the SZT ceramics increased due to the increase in density.



a



b

Fig. 4. a–dielectric constant; b–loss tangent with temperature (310–675 K) and frequency (0.1–1 MHz) of SZT ceramics microwave sintered at 950 °C

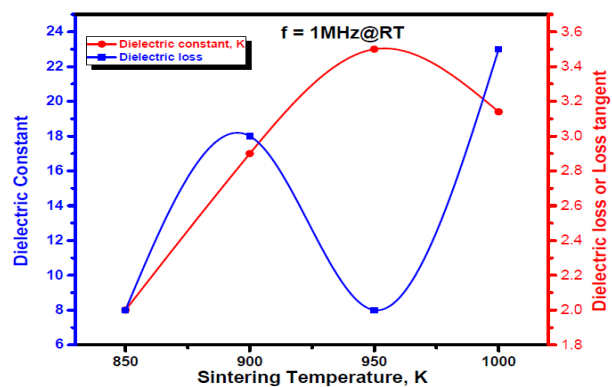


Fig. 5. Variation of dielectric constant and loss with the sintering temperature of SZT ceramics at RT and $f = 1$ MHz

As seen in Fig. 5, the SZT sample sintered at 950 °C has shown a high dielectric constant and low dielectric loss. This can be attributed to the imperfections that will work as scattering centers to the charge carriers and hence the huge value of dielectric constant and low dielectric loss may be obtained. The ionic radius of Sr^{2+} (1.12\AA) [31] is larger

compared to $Zn^{2+}(0.74\text{\AA})$ [22, 32], so the K was increased due to the increase of the dielectric polarizability of SZT samples with ilmenite structure [33].

4. CONCLUSIONS

In this work, a novel SZT nano-ceramic sample was synthesized successfully by the solid-state reaction method. We studied the effect of sintering temperature and environment on the dielectric properties of SZT ceramics. We found that the k of the SZT ceramics increased significantly and reached a maximum value of ~ 230 (0.1 KHz) at $950\text{ }^\circ\text{C}$ sintering temperature in microwave sintering. The dielectric constant is increased with temperature and decreased with frequency up to the transition temperature (650 K) of the samples. Therefore, tuning the sintering temperature can enhance the dielectric properties (high k and low $\tan(\delta)$) of SZT ceramics. This type of high k and low $\tan(\delta)$ values noticed at room temperature are most suitable for the filter, charge stored capacitors, and microwave resonator applications.

Acknowledgments

One of the authors, Dr. A. GuruSampath Kumar would like to acknowledge the Dept. of Physics, Sri Krishnadevaraya University, Anantapur, A.P. India-515003 for the support of experimental work in TSR labs.

REFERENCES

1. **Lei, S., Fan, H., Ren, X., Fang, J., Ma, L., Liu, Z.** Novel Sintering and Band Gap Engineering of Dielectric Properties *Journal of Materials Chemistry C* 5 2017: pp. 4040–4047. <https://doi.org/10.1039/C7TC00815E>
2. **Rao, B.H., Rao, A.V., Babu, K.S., Rao, G.N.** Low Temperature Investigation on Dielectric Properties of C Doped CuO *Ferroelectrics* 48 2021: pp. 46–55. <https://doi.org/10.1080/07315171.2021.1923120>
3. **Surendar, T., Kumar, S., Shankar, V.** Influence of La-doping on Phase Transformation and Photocatalytic Properties of ZnTiO₃ Nanoparticles Synthesized via Modified Sol-gel Method *Physical Chemistry & Chemical Physics* 16 2014: pp. 728–735. <https://doi.org/10.1039/c3cp53855a>
4. **Kumar, A.G.S., Obulapathi, L., Maddaiah, M., Sarmash, T.S., Rani, D.J., Rao, J.V.V.N.K., Rao, T.S., Asokan, K.** O₂-partial Pressure on the Physical Properties of DC-magnetron Sputtered Cadmium Zinc Oxide thin Films *AIP Conference Proceedings* 1665 2015: pp. 080002. <https://doi.org/10.1063/1.4917906>
5. **Sun, J., Xu, C., Zhao, X., Liang, J., Liao, R.** Improved Dielectric Properties of Indium and Tantalum Co-doped CaCu₃Ti₄O₁₂ Ceramic Prepared by Spark Plasma Sintering *IEEE Transactions on Dielectrics & Electrical Insulation* 27 2020: pp. 1400–1408. <https://doi.org/10.1109/TDEI.2020.008451>
6. **Chaouchi, A., Saidi, M., Astorg, S., Marinell, M.** Processing and Dielectric Properties of ZnTiO₃ Ceramics Prepared from Nanopowder Synthesised by Sol-Gel Technique *Processing & Applications of Ceramics* 6 2012: pp. 83–89. <https://doi.org/10.2298/PAC1202083C>
7. **Yim, K., Yong, Y., Lee, J., Lee, K., Nahm, L.H., Yoo, J., Lee, C.** Novel High- κ Dielectrics for Next-generation Electronic Devices Screened by Automated Ab Initio Calculations *NPG Asia Materials* 7 2015: pp. (e190)1–6. <https://doi.org/10.1038/am.2015.57>
8. **Kumar, P.S., Thyagarajan, K., Kumar, A.G., Obulapathi, L.** Investigations on Physical Properties of Mg Ferrite Nanoparticles for Microwave Applications *Journal of Microwave Power & Electromagnetic Energy* 53 2019: pp. 1–10. <https://doi.org/10.1080/08327823.2019.1569898>
9. **Wang, A.F.B., Huang, W., Chi, L., Al-Hashimi, M., Mark, T.J.** High- κ Gate Dielectrics for Emerging Flexible and Stretchable Electronics *Chemical Reviews* 118 2018: pp. 5690–5754. <https://doi.org/10.1021/acs.chemrev.8b00045>
10. **Samyuktha, V.S., Kumar, A.G.S., Suvarna, R.P.** Investigation of Electrical Aad Dielectric Studies of Calcium Doped Magnesium Titanate [Mg_(1-x)CaxTiO₃ (x=0–0.9)] ceramics *Digest Journal of Nanomaterials and Biostructures* 16 2021: pp. 839–846.
11. **Abirami, R., Kalaiselvi, C.R., Kungumadevi, L., Senthil, T.S., Kang, M.** Synthesis and Characterization of Zntio₃ and Ag-Doped Zntio₃ Perovskite Nanoparticles and Their Enhanced Photocatalytic and Antibacterial Activity *Journal of Solid State Chemistry* 281 2019: pp. 121019. <https://doi.org/10.1016/j.jssc.2019.121019>
12. **Maddaiah, M., Kumar, A.G., Sarmash, T.S., Naidu, K.C.B., Rani, D.J., Rao, T.S.** Synthesis and Characterization of Strontium Doped Zinc Manganese Titanate Ceramics *Digest Journal of Nanomaterials and Biostructures* 10 2015: pp. 155–159.
13. **Lin, L., Liu, Y., Zhang, J., Li, L., Lei, Z., Li, Y., Tian, M.** Enhancement of Breakdown Electric Field and Dielectric Properties of CaCu₃Ti₄O₁₂ ceramics by Sr doping *Materials Chemistry & Physics* 244 2020: pp. 122722. <https://doi.org/10.1016/j.matchemphys.2020.122722>
14. **Pallavi, S., Choudhary, P., Yadav, A., Rai, V.N., Mishra, A.** Effect of Strontium Doping on the Structural and Dielectric Properties of YCrO₃ *Journal of Materials Science: Materials in Electronics* 31 2020: pp. 12444–12454. <https://doi.org/10.1007/s10854-020-03791-z>
15. **Teoh, L.G., Lu, W., Lin, T.H., Lee, Y.** The Effect of Mg dopant and Oxygen Partial Pressure on Microstructure and Phase Transformation of ZnTiO₃ Thin Films *Journal of Nanomaterials* 2012 2012: pp. 1–8. <https://doi.org/10.1155/2012/539657>
16. **Ntwaeaborwa, O.M., Mofokeng, S.J., Kumar, V., Kroon, R.E., Cho, S.** Enhanced Red Emission of Eu in ZnO-TiO₂: Dy, Eu Nanocomposites by UV Down Conversion Process *Journal of Vacuum Science & Technology B* 37 2019: pp. 022901. <https://doi.org/10.1116/1.5081953>
17. **Rani, D.J., Kumar, A.G.S., Sarmash, T.S., Naidu, K.C.B., Maddaiah, M., Rao, T.S.** Effect of Argon/Oxygen Flow Rate Ratios on DC Magnetron Sputtered Nano-crystalline Zirconium Titanate Thin Films *JOM* 68 2016: pp. 1647–1652. <https://doi.org/10.1007/s11837-016-1910-5>
18. **Chaouchi, A., Astorg, S., Marinell, S., Aliouat, M.** ZnTiO₃ Ceramic Sintered at Low Temperature with Glass Phase Addition for LTCC Applications *Materials Chemistry & Physics* 103 2007: pp. 106–111. <https://doi.org/10.1016/j.matchemphys.2007.01.017>
19. **Chai, Y., Chang, Y., Chen, G., Hsiao, Y.** The Effects of Heat-treatment on the Structure Evolution and Crystallinity of

- ZnTiO₃ Nano-crystals Prepared by Pechini Process *Materials Research Bulletin* 43 2008: pp. 1066–1073.
<https://doi.org/10.1016/j.materresbull.2007.06.002>
20. **Kumar, A.G.S., Xuejin, L., Du, Y., Geng, Y., Hong, X.** UV-light Enhanced High Sensitive Hydrogen (H₂) Sensor Based on Spherical Au Nanoparticles on ZnO Nano-structured Thin Films *Journal of Alloys & Compounds* 798 2019: pp. 467–477.
<https://doi.org/10.1016/j.jallcom.2019.05.227>
 21. **Kumar, A.G.S., Sarmash, T.S., Rani, D.J., Obulapathi, L., Rao, G.V.V.B., Rao, T.S., Asokan, K.** Effect of Post Sputter Annealing Treatment On Nano-Structured Cadmium Zinc Oxide Thin Films *Journal of Alloys & Compounds* 665 2016: pp. 86–92.
<https://doi.org/10.1016/j.jallcom.2016.01.029>
 22. **Dubey, R.S., Jadkar, S.R., Bhorde, A.B.** Synthesis and Characterization of Various Doped TiO₂ Nanocrystals for Dye-sensitized Solar Cells *ACS Omega* 6 2021: pp. 3470–3482.
<https://doi.org/10.1021/acsomega.0c01614>
 23. **Liu, S., Wang, H., Wang, H.** Effect of Grinding Time on The Particle Size Distribution Characteristics of Tuff Powder *Materials Science (Medziagotyra)* 27 (2) 2021: pp. 205–209.
<http://dx.doi.org/10.5755/j02.ms.23526>
 24. **Babu, S.J., Rao, V.N., Murhy, D.H.K., Shastri, M., Murthy, M., Shetty, M., Raju, K.S.A., Shivaramu, P.D., Kumar, C.S.A., Shankar, M.V., Rangappa, D.** Significantly Enhanced Cocatalyst-Free H₂ Evolution from Defect-engineered Brown TiO₂ *Ceramics International* 47 2021: pp. 14821–14828.
<https://doi.org/10.1016/j.ceramint.2020.10.026>
 25. **Kim, E.S., Jeon, C.J.** Microwave Dielectric Properties of ATiO₃ (A = Ni, Mg, Co, Mn) Ceramics *Journal of European Ceramic Society* 30 2010: pp. 341–346.
<https://doi.org/10.1016/j.jeurceramsoc.2009.08.017>
 26. **Kumar, P.S., Thyagarajan, K., Kumar, A.G.** Investigations on Physical Properties of Zn Ferrite Nanoparticles Using Sol-gel Auto Combustion Technique *Digest Journal of Nanomaterials and Biostructures* 13 2018: pp. 1117–1122.
 27. **Rao, B.H., Rao, A.V., Kumar, A.G.S., Rao, G.N.** Investigation of Low Temperature Dielectric Properties of Manganese Doped-copper Oxide Nanoparticles by Coprecipitation Method *Digest Journal of Nanomaterials and Biostructures* 16 (3) 2021: pp. 1173–1183.
 28. **Okhay, O., Vilarinho, P.M., Tkach, A.** Low-temperature Dielectric Response of Strontium Titanate Thin Films Manipulated by Zn Doping *Materials* 15 2022: pp. 859.
<https://doi.org/10.3390/ma15030859>
 29. **Chang, Y., Chang, Y., Chen, L., Chen, G., Chai, Y., Fang, T., Wu, S.** Synthesis, Formation and Characterization of ZnTiO₃ Ceramics *Ceramics International* 30 2004: pp. 2183–2189.
<https://doi.org/10.1016/j.ceramint.2004.01.002>
 30. **Rani, D.J., Kumar, A.G.S., Obulapathi, L., Rao, T.S.** Dielectric and Optical Properties of Zirconium Titanate Thin Films by Reactive DC Magnetron Co-sputtering *IEEE Transactions on Dielectrics and Electrical Insulation* 26 2019: pp. 1134–1138.
<https://doi.org/10.1109/TDEI.2019.007887>
 31. **Kumar, A.G., Sarmash, T.S., Obulapathi, L., Rani, D.J., Rao, T.S., Asokan, K.** Structural, Optical and Electrical Properties of Heavy Ion Irradiated CdZnO Thin Films *Thin Solid Films* 605 2016: pp. 102–107.
<https://doi.org/10.1016/j.tsf.2015.12.024>
 32. **Samyuktha, V.S., Kumar, A.G., Rao, T.S., Suvarna, R.P.** Synthesis, Structural and Dielectric Properties of Magnesium Calcium Titanate (1-x)MgTiO_{3-x}CaTiO₃ (x=0, 0.1, 0.2 and 0.3) *Materials Today:Proceedings* 3 2016: pp. 1768–1771.
<https://doi.org/10.1016/j.matpr.2016.04.072>



© Ankisetty et al. 2023 Open Access This article is distributed under the terms of the Creative Commons Attribution 4.0 International License (<http://creativecommons.org/licenses/by/4.0/>), which permits unrestricted use, distribution, and reproduction in any medium, provided you give appropriate credit to the original author(s) and the source, provide a link to the Creative Commons license, and indicate if changes were made.